

# How rapidly do neutron stars spin at birth? Constraints from archival X-ray observations of extragalactic supernovae

Rosalba Perna<sup>1</sup>, Roberto Soria<sup>2</sup>, Dave Pooley<sup>3</sup>, Luigi Stella<sup>4</sup>

<sup>1</sup> *JILA and Department of Astrophysical and Planetary Sciences, University of Colorado, Boulder, CO, 80309*

<sup>2</sup> *MSSL, University College London, Holmbury St Mary, Dorking RH5 6NT, UK*

<sup>3</sup> *Astronomy Department, University of Wisconsin-Madison 475 North Charter st., Madison, WI 53706, USA*

<sup>4</sup> *INAF - Osservatorio Astronomico di Roma, Via Frascati 33, I-00040 Rome, Italy*

1 November 2018

## ABSTRACT

Traditionally, studies aimed at inferring the distribution of birth periods of neutron stars are based on radio surveys. Here we propose an independent method to constrain the pulsar spin periods at birth based on their X-ray luminosities. In particular, the observed luminosity distribution of supernovae poses a constraint on the initial rotational energy of the embedded pulsars, via the  $L_X - \dot{E}_{\text{rot}}$  correlation found for radio pulsars, and under the assumption that this relation continues to hold beyond the observed range. We have extracted X-ray luminosities (or limits) for a large sample of historical SNe observed with *Chandra*, *XMM* and *Swift*, that have been firmly classified as core-collapse supernovae. We have then compared these observational limits with the results of Monte Carlo simulations of the pulsar X-ray luminosity distribution, for a range of values of the birth parameters. We find that a pulsar population dominated by millisecond periods at birth is ruled out by the data.

## 1 INTRODUCTION

Modeling the observed properties of the Galactic population of radio pulsars, with the purpose of inferring their intrinsic properties, has been the subject of extensive investigation for several decades (e.g. Gunn & Ostriker 1970; Phinney & Blandford 1981; Lyne et al. 1985; Stollman 1987; Emmering & Chevalier 1989; Narayan & Ostriker 1990; Lorimer et al. 1993; Hartman et al. 1997; Cordes & Chernoff 1998; Arzoumanian, Cordes & Chernoff 2002; Vranesevic et al 2004; Faucher-Giguere & Kaspi 2006; Ferrario & Wickramasinghe 2006). Since the fraction of pulsars that can be detected close to their birth constitutes a negligible fraction of the total sample, these studies generally use the *present day* observed properties of pulsars (namely their period  $P$  and period derivative  $\dot{P}$ ), together with some assumptions about their time evolution, to reconstruct the birth distribution of periods and magnetic fields for the pulsar population. These analyses also need to make assumptions about pulsar properties and their evolution (such as, for example, the exact shape of the radio beam and its dependence on the period), as well as overcome a number of selection effects. Results from various investigations have often been conflicting, with some studies favoring initial periods in the millisecond range (e.g. Arzoumanian et al. 2002), and others instead finding more likely periods in the range of several tens to several hundreds of milliseconds (e.g. Faucher-

Giguere & Kaspi 2006). The efforts put over the years into this area of research stem from the fact that the birth properties of neutron stars (NSs) are intimately related to the physical processes occurring during the supernova (SN) explosion and in the proto-neutron star. As such, they bear crucial information on the physics of core-collapse SNe, in which most are thought to be formed.

Besides the inferences on the birth parameters from the radio population discussed above, we show here that constraints can be derived also from the X-rays. Young, fast rotating neutron stars are indeed expected to be very bright in the X-rays. In fact, observationally there appears to be a correlation between the rotational energy loss of the star,  $\dot{E}_{\text{rot}}$ , and its X-ray luminosity,  $L_x$ . This correlation was noticed by Verbunt et al. (1996), Becker & Trumper (1997), Seward & Wang (1988), Saito (1998) for a small sample of objects, and later studied by Possenti et al. (2002; P02 in the following) for the largest sample of pulsars known to date.

Combining the birth parameters derived from the radio (which determine the birth distribution of  $\dot{E}_{\text{rot}}$  for the pulsars), with the empirical  $L_x - \dot{E}_{\text{rot}}$  correlation, the distribution of X-ray luminosity can be predicted for a sample of pulsars with a certain age distribution. The above calculation was performed by Perna & Stella (2004). They found that the birth parameters derived by Arzoumanian et al. (2002), together with the  $L_x - \dot{E}_{\text{rot}}$  correlation derived by P02, yield a sizable fraction of sources with luminosities

$\gtrsim 10^{39}$  erg/s, which could hence constitute potential contributors to the observed population of ultra luminous X-ray sources (ULXs) observed in nearby galaxies (e.g. Fabbiano & White 2003; Ptak & Colbert 2004). Obviously, these predictions were heavily dependent on the assumed initial birth parameters (the periods especially) of the pulsar population.

In this paper, we propose a new, independent method to constrain the pulsar spin periods at birth from X-ray observations, and hence also assess the contribution of young, fast rotating NSs to the population of bright X-ray sources. Since neutron stars are born in supernova explosions, and very young pulsars are still embedded in their supernovae, the X-ray luminosity of the SNe provides an upper limit to the luminosity of the embedded pulsars. We have analyzed an extensive sample of historical SNe whose position has been observed by *Chandra*, *XMM* or *Swift*, and studied their X-ray counterparts. We measured their X-ray luminosities, or derived a limit on them in the cases of no detection. A comparison between these limits and the theoretical predictions for the distribution of pulsar X-ray luminosities shows that, if the assumed initial spins are in the millisecond range, the predicted distribution of pulsar X-ray luminosities via the  $L_x - \dot{E}_{\text{rot}}$  correlation is highly inconsistent with the SN data. Our analysis hence suggests that a substantial fraction of pulsars cannot be born with millisecond periods.

The paper is organized as follows: in §2, we describe the method by which the SN X-ray flux measurements and limits are extracted, while in §3 we describe the theoretical model for the distribution of the X-ray luminosity of young pulsars. A comparison between the theoretical predictions and the data is performed in §4, while the results are summarized and discussed in §5.

## 2 X-RAY ANALYSIS OF HISTORICAL SUPERNOVAE OBSERVED BY *CHANDRA*, *XMM* AND *SWIFT*

We compared and combined the CfA List of Supernovae<sup>1</sup>, the Padova-Asiago Catalogue<sup>2</sup>, the Sternberg Catalogue<sup>3</sup> (Tsvetkov et al. 2004), and Michael Richmond's Supernova Page<sup>4</sup>, to create a list of unambiguously identified core-collapse SNe (updated to 2007 April). We cross-correlated the SN positions with the catalogues of *Chandra*/ACIS, *XMM-Newton*/EPIC and *Swift*/XRT observations<sup>5</sup>, to determine which SN fields have been observed by recent X-ray missions (*ASCA* was excluded because of its low spatial resolution, and *ROSAT* because of its lack of 2–10 keV sensitivity). For the *Chandra* ACIS-S data, we limited our search to the S3 chip. We obtained a list of  $\sim 200$  core-collapse SNe whose positions happened to be in a field observed at least once after the event. From the list, we then selected for this paper all the core collapse SNe with unambiguous subtype classification (Type Ib/c, Type IIIn, IIL, and IIP and IIb).

<sup>1</sup> <http://cfa-www.harvard.edu/iau/lists/Supernovae.html>, compiled by The Central Bureau for Astronomical Telegrams at the Harvard-Smithsonian Center for Astrophysics.

<sup>2</sup> <http://web.pd.astro.it/supern/snean.txt>

<sup>3</sup> VizieR On-line Data Catalog: II/256

<sup>4</sup> <http://stupendous.rit.edu/richmond/sne/sn.list>

<sup>5</sup> Search form at <http://heasarc.nasa.gov>

That is about half of the total sample. We leave the analysis of the other  $\sim 100$  SNe (classified generically as Type II) to a follow-up paper.

We retrieved the relevant X-ray datasets from the public archives of those three missions. The optical position of each SN in our sample is well known, to better than  $1''$ : this makes it easier to determine whether a SN is detected in the X-ray band (in particular for *Chandra*), even with a very low number of counts, at a level that would not be considered significant for source detection in a blind search. For the *Chandra* observations, we applied standard data analysis routines within the Chandra Interactive Analysis of Observations (CIAO) software package<sup>6</sup> version 3.4. Starting from the level-2 event files, we defined a source region (radius  $2'5$ , comprising  $\approx 95\%$  of the source counts at 2 keV, on axis, and proportionally larger extraction radii for off-axis sources) and suitable background regions not contaminated by other sources and at similar distances from the host galaxy's nucleus. For each SN, we extracted source and background counts in the 0.3–8 keV band with *dmextract*. In most cases, we are dealing with a very small number of counts (e.g., 2 or 3, inside the source extraction region) and there is no excess of counts at the position of the SN with respect to the local background. In these cases, we calculated the 90% upper limit to the number of net counts with the Bayesian method of Kraft et al. (1991). We then converted this net count-rate upper limit to a flux upper limit with WebPimms<sup>7</sup>, assuming a power-law spectral model with photon index  $\Gamma = 2$  and line-of-sight Galactic column density. The choice of a power-law spectral model is motivated by our search for X-ray emission from an underlying pulsars rather than from the SN shock wave. In a few cases, there is a small excess of counts at the SN position: we then also built response and auxiliary response functions (applying *psextract* in CIAO), and used them to estimate a flux, assuming the same spectral model. When possible, for sources with  $\approx 20$ –100 net counts, we determined the count rates separately in the soft (0.3–1 keV), medium (1–2 keV) and hard (2–8 keV) bands, and used the hard-band rates (essentially uncontaminated by soft thermal-plasma emission, and unaffected by the uncertainty in the column density and by the degradation of the ACIS-S sensitivity) alone to obtain a more stringent value or upper limit to the non-thermal power-law emission. Very few sources have enough counts for a two-component spectral fit (mekal thermal plasma plus power-law): in those cases, we used the 2–10 keV flux from the power-law component alone in the best-fitting spectral model. For those spectral fits, we used the XSPEC version 12 software package (Arnaud 1996).

When we had to rely on *XMM-Newton*/EPIC data, we followed essentially the same scheme: we estimated source and background count rates (this time, using a source extraction circle with a  $20''$  radius) in the full EPIC pn and MOS bands (0.3–12 keV) and, when possible, directly in the 2–10 keV band. The count rate to flux conversion was obtained with WebPimms (with a  $\Gamma = 2$  power-law model absorbed by line-of-sight column density) or through full spec-

<sup>6</sup> <http://cxc.harvard.edu/ciao>

<sup>7</sup> <http://heasarc.nasa.gov/Tools/w3pimms.html> and <http://cxc.harvard.edu/toolkit/pimms.jsp>

SN	Host galaxy	Type	Age (yr)	$L_{2-10 \text{ keV}}$ (erg/s)	Instrument	Observation date
1923A	N5236	IIP	77.3	$< 6.0 \times 10^{35}$	ACIS	2000-04-29, 2001-09-04
1926A	N4303	IIP	75.3	$< 1.4 \times 10^{37}$	ACIS	2001-08-07
1937A	N4157	IIP	67.3	$< 1.3 \times 10^{37}$	EPIC	2004-05-16
1937F	N3184	IIP	62.1	$< 2.7 \times 10^{36}$	ACIS	2000-01-08, 2000-02-03
1940A	N5907	IIL	63.0	$< 1.0 \times 10^{37}$	EPIC	2003-02-20, 2003-02-28
1940B	N4725	IIP	62.6	$< 8.6 \times 10^{36}$	ACIS	2002-12-02
1941A	N4559	IIL	60.2	$< 5.5 \times 10^{36}$	ACIS	2001-01-14, 2001-06-04, 2002-03-14
1948B	N6946	IIP	55.1	$< 4.7 \times 10^{35}$	ACIS	2001-09-07, 2002-11-25, 2004-10-22, 2004-11-06, 2004-12-03
1954A	N4214	Ib	48.9	$< 1.6 \times 10^{35}$	ACIS	2003-03-09
1959D	N7331	IIL	41.6	$< 2.2 \times 10^{37}$	ACIS	2001-01-27
1961V	N1058	IIn	38.3	$< 6.1 \times 10^{37}$	ACIS	2000-03-20
1962L	N1073	Ic	41.2	$< 4.7 \times 10^{37}$	ACIS	2004-02-09
1962M	N1313	IIP	40.3	$< 3.7 \times 10^{35}$	ACIS	2002-10-13, 2002-11-09, 2003-10-02, 2004-02-22
1965H	N4666	IIP	37.7	$< 1.5 \times 10^{38}$	ACIS	2003-02-14
1965L	N3631	IIP	37.8	$< 5.7 \times 10^{36}$	ACIS	2003-07-05
1968L	N5236	IIP	32.0	$< 1.5 \times 10^{36}$	ACIS	2000-04-29, 2001-09-04
1969B	N3556	IIP	32.6	$< 3.8 \times 10^{36}$	ACIS	2001-09-08
1969L	N1058	IIP	30.3	$< 4.8 \times 10^{37}$	ACIS	2000-03-20
1970G	N5457	IIL	33.9	$< 4.9 \times 10^{36}$	ACIS	2004-07-05, 2004-07-11
1972Q	N4254	IIP	30.5	$< 3.0 \times 10^{38}$	EPIC	2003-06-29
1972R	N2841	Ib	31.9	$< 7.3 \times 10^{35}$	EPIC	2004-11-09
1973R	N3627	IIP	25.9	$< 7.7 \times 10^{37}$	ACIS	1999-11-03
1976B	N4402	Ib	26.2	$< 8.9 \times 10^{37}$	EPIC	2002-07-01
1979C	N4321	IIL	26.8	$2.7^{+0.4}_{-0.4} \times 10^{38}$	ACIS	2006-02-18
1980K	N6946	IIL	24.0	$< 6.5 \times 10^{36}$	ACIS	2004-10-22, 2004-11-06, 2004-12-03
1982F	N4490	IIP	22.6	$< 1.1 \times 10^{36}$	ACIS	2004-07-29, 2004-11-20
1983E	N3044	IIL	19.0	$< 4.6 \times 10^{37}$	EPIC	2001-11-24, 2002-05-10
1983I	N4051	Ic	17.8	$< 1.7 \times 10^{36}$	ACIS	2001-02-06
1983N	N5236	Ib	16.8	$< 5.5 \times 10^{36}$	ACIS	2000-04-29
1983V	N1365	Ic	19.1	$< 7.0 \times 10^{37}$	ACIS	2002-12-24
1985L	N5033	IIL	14.9	$< 8.1 \times 10^{37}$	ACIS	2000-04-28
1986E	N4302	IIL	19.6	$1.4^{+0.5}_{-0.5} \times 10^{38}$	ACIS	2005-12-05
1986I	N4254	IIP	17.1	$< 3.0 \times 10^{38}$	EPIC	2003-06-29
1986J	N891	IIn	21.2	$8.5^{+0.5}_{-0.5} \times 10^{38}$	ACIS	2003-12-10
1986L	N1559	IIL	18.9	$< 1.4 \times 10^{38}$	EPIC	2005-08-10, 2005-10-12
1987B	N5850	IIn	14.1	$< 1.5 \times 10^{38}$	EPIC	2001-01-25, 2001-08-26
1988A	N4579	IIP	12.3	$< 2.4 \times 10^{37}$	ACIS	2000-05-02
1988Z	MCG+03-28-22	IIn	15.5	$2.9^{+0.5}_{-0.5} \times 10^{39}$	ACIS	2004-06-29
1990U	N7479	Ic	10.9	$1.1^{+0.6}_{-0.5} \times 10^{39}$	EPIC	2001-06-19
1991N	N3310	Ib/Ic	11.8	$< 4.2 \times 10^{37}$	ACIS	2003-01-25
1993J	N3031	I Ib	8.1	$< 1.0 \times 10^{38}$	ACIS	2001-04-22
1994I	N5194	Ic	8.2	$8.0^{+0.3}_{-0.7} \times 10^{36}$	ACIS	2000-06-20, 2001-06-23, 2003-08-07
1994ak	N2782	IIn	7.4	$< 3.7 \times 10^{37}$	ACIS	2002-05-17
1995N	MCG-02-38-17	IIn	8.9	$4.3^{+1.0}_{-1.0} \times 10^{39}$	ACIS	2004-03-27
1996ae	N5775	IIn	5.9	$< 6.1 \times 10^{37}$	ACIS	2002-04-05
1996bu	N3631	IIn	6.6	$< 2.1 \times 10^{37}$	ACIS	2003-07-05
1996cr	ESO97-G13	IIn	4.2	$1.9^{+0.4}_{-0.4} \times 10^{39}$	ACIS	2000-03-14
1997X	N4691	Ic	6.1	$< 2.2 \times 10^{37}$	ACIS	2003-03-08
1997bs	N3627	IIn	2.5	$< 2.9 \times 10^{38}$	ACIS	1999-11-03
1998S	N3877	IIn	3.6	$3.8^{+0.5}_{-0.5} \times 10^{39}$	ACIS	2001-10-17
1998T	N3690	Ib	5.2	$< 2.0 \times 10^{38}$	ACIS	2003-04-30
1998bw	ESO184-G82	Ic	3.5	$4.0^{+1.0}_{-0.9} \times 10^{38}$	ACIS	2001-10-27
1999dn	N7714	Ib	4.4	$< 5.9 \times 10^{37}$	ACIS	2004-01-25
1999ec	N2207	Ib	5.9	$3.1^{+0.4}_{-0.4} \times 10^{39}$	EPIC	2005-08-31
1999el	N6951	IIn	5.6	$< 5.6 \times 10^{38}$	EPIC	2005-04-30, 2005-06-05
1999em	N1637	IIP	1.0	$< 1.4 \times 10^{37}$	ACIS	2000-10-30
1999gi	N3184	IIP	0.10	$2.6^{+0.6}_{-0.6} \times 10^{37}$	ACIS	2000-01-08, 2000-02-03
2000P	N4965	IIn	7.2	$< 1.2 \times 10^{39}$	XRT	2007-05-16
2000bg	N6240	IIn	1.3	$< 1.4 \times 10^{39}$	ACIS	2001-07-29
2001ci	N3079	Ic	2.5	$< 5.0 \times 10^{37}$	EPIC	2003-10-14
2001du	N1365	IIP	1.3	$< 3.8 \times 10^{37}$	ACIS	2002-12-24
2001em	UGC11794	Ib/Ic	4.7	$5.8^{+1.2}_{-1.2} \times 10^{40}$	EPIC	2006-06-14
2001gd	N5033	I Ib	1.1	$1.0^{+0.3}_{-0.3} \times 10^{39}$	EPIC	2002-12-18
2001ig	N7424	I Ib	0.50	$3.5^{+2.0}_{-2.0} \times 10^{37}$	ACIS	2002-06-11

SN	Host galaxy	Type	Age (yr)	$L_{2-10 \text{ keV}}$ (erg/s)	Instrument	Observation date
2002ap	N628	Ic	0.92	$< 3.1 \times 10^{36}$	EPIC	2003-01-07
2002fj	N2642	IIn	4.7	$< 1.3 \times 10^{39}$	XRT	2007-05-11
2002hf	MCG-05-3-20	Ic	3.1	$< 7.6 \times 10^{38}$	EPIC	2005-12-19
2003L	N3506	Ic	0.08	$7.7^{+1.5}_{-1.5} \times 10^{39}$	ACIS	2003-02-10
2003ao	N2993	IIP	0.016	$5.6^{+1.2}_{-1.2} \times 10^{38}$	ACIS	2003-02-16
2003bg	MCG-05-10-15	Ic/IIfb	0.33	$5.3^{+1.3}_{-0.8} \times 10^{38}$	ACIS	2003-06-22
2003dh	Anon.	Ic	0.71	$< 5.0 \times 10^{40}$	EPIC	2003-12-12
2003jd	MCG-01-59-21	Ic	0.041	$< 3.0 \times 10^{38}$	ACIS	2003-11-10
2003lw	Anon.	Ic	0.34	$7.0^{+3}_{-3} \times 10^{40}$	ACIS	2004-04-18
2004C	N3683	Ic	3.1	$1.0^{+0.3}_{-0.2} \times 10^{38}$	ACIS	2007-01-31
2004dj	N2403	IIP	0.34	$1.1^{+0.3}_{-0.3} \times 10^{37}$	ACIS	2004-12-22
2004dk	N6118	Ib	0.030	$1.5^{+0.4}_{-0.4} \times 10^{39}$	EPIC	2004-08-12
2004et	N6946	IIP	0.18	$1.0^{+0.2}_{-0.2} \times 10^{38}$	ACIS	2004-10-22, 2004-11-06, 2004-12-03
2005N	N5420	Ib/Ic	0.50	$< 1.0 \times 10^{40}$	XRT	2005-07-17
2005U	Anon.	IIfb	0.041	$< 1.1 \times 10^{39}$	ACIS	2005-02-14
2005at	N6744	Ic	1.7	$< 3.0 \times 10^{38}$	XRT	2006-10-31
2005bf	MCG+00-27-5	Ib	0.58	$< 6.0 \times 10^{39}$	XRT	2005-11-07
2005bx	MCG+12-13-19	IIn	0.25	$< 1.0 \times 10^{39}$	ACIS	2005-07-30
2005da	UGC11301	Ic	0.098	$< 5.0 \times 10^{39}$	XRT	2005-08-23
2005db	N214	IIn	0.036	$< 2.0 \times 10^{39}$	EPIC	2005-08-01
2005ek	UGC2526	Ic	0.041	$< 4.0 \times 10^{39}$	XRT	2005-10-07
2005gl	N266	IIn	1.6	$< 3.4 \times 10^{39}$	XRT	2007-06-01
2005kd	Anon.	IIn	1.2	$2.6^{+0.4}_{-0.4} \times 10^{41}$	ACIS	2007-01-24
2006T	N3054	IIfb	0.0082	$< 6.0 \times 10^{39}$	XRT	2006-02-02
2006aj	Anon.	Ic	0.43	$< 7.0 \times 10^{39}$	XRT	2006-07-25
2006bp	N3953	IIP	0.058	$1.0^{+0.2}_{-0.2} \times 10^{38}$	EPIC	2006-04-30
2006bv	UGC7848	IIn	0.0082	$< 1.2 \times 10^{39}$	XRT	2006-05-01
2006dn	UGC12188	Ib	0.033	$< 2.5 \times 10^{40}$	XRT	2006-07-17
2006gy	N1260	IIn	0.16	$< 2.0 \times 10^{38}$	ACIS	2006-11-15
2006jc	UGC4904	Ib	0.068	$2.1^{+0.6}_{-0.6} \times 10^{38}$	ACIS	2006-11-04
2006lc	N7364	Ib/Ic	0.016	$< 2.0 \times 10^{40}$	XRT	2006-10-27
2006lt	Anon.	Ib	0.068	$< 4.0 \times 10^{39}$	XRT	2006-11-05
2007C	N4981	Ib	0.022	$< 3.0 \times 10^{40}$	XRT	2007-01-15
2007D	UGC2653	Ic	0.025	$< 3.0 \times 10^{40}$	XRT	2007-01-18
2007I	Anon.	Ic	0.016	$< 9.0 \times 10^{39}$	XRT	2007-01-20
2007bb	UGC3627	IIn	0.022	$< 4.4 \times 10^{39}$	XRT	2007-04-10

**Table 1.** X-ray measurements and upper limits for our sample of historical supernovae. When more than one observation was used for a given source, the age is an average of three epochs weighted by their exposure lengths. The instrument ACIS is on-board *Chandra*, EPIC on *XMM-Newton* and XRT on *Swift*.

tral analysis for sources with enough counts. We used standard data analysis tasks within the Science Analysis System (SAS) version 7.0.0 (for example, *xmmselect* for source extraction). All three EPIC detectors were properly combined, both when we estimated count rates, and when we did spectral fitting, to increase the signal-to-noise ratio. In fact, in almost all cases in which a source position had been observed by both *Chandra* and *XMM-Newton*, *Chandra* provided a stronger constraint to the flux, because of its much narrower point-spread function and lower background noise. The *Swift* data were analyzed using the Swift Software version 2.3 tools and latest calibration products. Source counts were extracted from a circular region with an aperture of  $20''$  radius centered at the optical positions of the SNe. In some cases, Swift observations referred to a Gamma ray burst (GRB) associated to a core-collapse SN: we did not obviously consider the GRB flux for our population analysis. Instead, for those cases, we considered the most recent *Swift* observation after the GRB had faded, and used that to determine an upper limit to a possible pulsar emission. We

only considered *Swift* observations deep enough to detect or constrain the residual luminosity to  $\lesssim 10^{40}$  erg s $^{-1}$ .

In some cases, two or more *Chandra* or *XMM-Newton* observations of the same SN target were found in the archive. If they were separated by a short interval in time (much shorter than the time elapsed from the SN explosion), we merged them together, to increase the detection threshold. The reason we can do this is that we do not expect the underlying pulsar luminosity to change significantly between those observations. However, when the time elapsed between observations was comparable to the age of the SN, we attributed greater weight to the later observations, for our flux estimates. The reason is that the thermal X-ray emission from the shocked gas tends to decline more rapidly (over a few months or years) than the non-thermal pulsar emission (timescale  $\gtrsim$  tens of years). More details about the data analysis and the luminosity and color/spectral properties of individual SNe in our sample will be presented elsewhere (Pooley et al. 2008, in preparation). Here, we are mainly interested in a population study to constrain the possible

presence and luminosity of high-energy pulsars detectable in the 2–10 keV band.

While this is, to the best of our knowledge, the first X-ray search for pulsar wind nebulae (PWNe) in extragalactic SNe, and the first work that uses these data to set statistical constraints on the properties of the embedded pulsars, it should be noted that the possibility of observing pulsars in young SNe (a few years old) was originally discussed, from a theoretical point of view, by Chevalier & Fransson (1992). Furthermore, searches for PWNe in extragalactic SNe have been performed in the radio (Reynolds & Fix 1987; Bartel & Bietenholz 2005). Observationally, however, clear evidence for pulsar activity in SNe has been lacking. The radio emission detected in some SNe, although initially ascribed to pulsar activity (Bandiera, Pacini & Salvati 1984), was later shown to be well described as the result of circumstellar interaction (Lundqvist & Fransson 1988). There is however a notable exception, that is SN 1986J, for which the observed temporal decline of the  $H_\alpha$  luminosity (Rupen et al. 1987) has been considered suggestive of a pulsar energy input (Chevalier 1987). As noted by Chevalier (1989), a possible reason for the apparent low-energy input in some cases could be the fact that the embedded neutron stars were born with a relatively long period. The present work allows us to make a quantitative assessment on the typical minimum periods allowed for the bulk of the NS population. The list of SNe, their measured fluxes and their ages (at the time of observation) are reported in Table 1.

### 3 THEORETICAL EXPECTATIONS FOR THE X-RAY LUMINOSITY OF YOUNG PULSARS

Most isolated neutron stars are X-ray emitters throughout all their life: at early times, their X-ray luminosity is powered by rotation (e.g. Michel 1991; Becker & Trumper 1997); after an age of  $\sim 10^3 - 10^4$  yr, when the star has slowed down sufficiently, the main X-ray source becomes the internal heat of the star<sup>8</sup>, and finally, when this is exhausted, the only possible source of X-ray luminosity would be accretion by the interstellar medium, although to a very low luminosity level, especially for the fastest stars (e.g. Blaes & Madau 1993; Popov et al. 2000; Perna et al. 2003). Another possible source of X-ray luminosity that has often been discussed in the context of NSs is accretion from a fallback disk (Colgate 1971; Michel & Dressler 1981; Chevalier 1989; Yusifov et al. 1995; Chatterjee et al. 2000; Alpar 2001; Perna et al. 2000). Under these circumstances, accretion would turn off magnetospheric emission, and X-ray radiation would be produced as the result of accretion onto the surface of the star. For a disk to be able to interfere with the magnetosphere and accrete, the magnetospheric radius  $R_m \sim 6.6 \times 10^7 B_{12}^{4/7} \dot{m}^{-2/7}$  cm (with  $\dot{m}^{-2/7}$  being the accretion rate in Eddington units, and  $B_{12} \equiv B/(10^{12}\text{G})$ ) must be smaller than the corotation radius  $R_{\text{cor}} \sim 1.5 \times 10^8 P^{2/3} (M/M_\odot)^{1/3}$  cm. If, on the other hand, the magnetospheric radius resides outside of the corotation radius, the propeller effect (Illarionov & Sunyaev

1975) takes over and inhibits the penetration of material inside the magnetosphere, and accretion is (at least largely) suppressed. For a typical pulsar magnetic field  $B_{12} \sim 5$ , the magnetospheric radius becomes comparable to the corotation radius for a period  $P \sim 1$  s and an Eddington accretion rate. If the infalling material does not possess sufficient angular momentum, however, a disk will not form, but infall of the bound material from the envelope is still likely to proceed, albeit in a more spherical fashion. The accretion rate during the early phase depends on the details of the (yet unclear) explosion mechanism. Estimates by Chevalier (1989) yield values in the range  $3 \times 10^{-4} - 2 \times 10^2 M_\odot \text{ yr}^{-1}$ . In order for the pulsar mechanism to be able to operate, the pressure of the pulsar magnetic field must overcome that of the spherical infall. For the accretion rates expected at early times, however, the pressure of the accreting material dominates over the pulsar pressure even at the neutron star surface. Chevalier (1989) estimates that, for accretion rates  $\dot{M} \gtrsim 3 \times 10^{-4} M_\odot \text{ yr}^{-1}$ , the photon luminosity is trapped by the inflow and the effects of a central neutron star are hidden. Once the accretion rate drops below that value, photons begin to diffuse out from the shocked envelope; from that point on, the accretion rate drops rapidly, and the pulsar mechanism can turn on. Chevalier (1989) estimates that this occurs at an age of about 7 months. Therefore, even if fallback plays a major role in the initial phase of the SN and NS lives, its effects are not expected to be relevant at the timescales of interest for the conclusions of this work.

For the purpose of our analysis, we are especially interested in the X-ray luminosity at times long enough so that accretion is unimportant, but short enough that rotation is still the main source of energy. During a Crab-like phase, relativistic particles accelerated in the pulsar magnetosphere are fed to a synchrotron emitting nebula, the emission of which is characterized by a powerlaw spectrum. Another important contribution is the pulsed X-ray luminosity (about 10% of the total in the case of the Crab) originating directly from the pulsar magnetosphere. It should be noted that one important assumption of our analysis is that all (or at least the greatest majority) of neutron stars goes through an early time phase during which their magnetosphere is active and converts a fraction of the rotational energy into X-rays. However, there is observational evidence that there are objects, known as Central Compact Objects<sup>9</sup> (CCOs), for which no pulsar wind nebulae are detected. Since no pulsations are detected for these stars, it is possible that they are simply objects born slowly rotating and which hence have a low value of  $\dot{E}_{\text{rot}}$ . In this case, they would not affect any of our considerations, since the  $L_x - \dot{E}_{\text{rot}}$  correlation appears to hold all the way down to the lowest measured values of  $L_x$  and  $\dot{E}_{\text{rot}}$ . However, if the CCOs are NSs with a high  $\dot{E}_{\text{rot}}$ , but for which there exists some new physical mechanism that suppresses the magnetospheric activity (and hence the X-ray luminosity) to values much below what allowed by the scatter in the pulsar  $L_x - \dot{E}_{\text{rot}}$  relation, then these stars would affect the limits that we derive. Since at this stage their nature is uncertain, we treat the all sample of NSs on the same footing, although keeping this in mind as a

<sup>8</sup> In the case of magnetars, this internal heat is provided by magnetic field decay, which dominates over all other energy losses.

<sup>9</sup> Examples are central source in Cas A and in Puppis A (e.g. Petre et al. 1996; Pavlov et al. 2000).

caveat should future work demonstrate the different intrinsic nature of the CCOs with respect to the conversion of rotational energy into X-ray luminosity.

As discussed in §1, for all the neutron stars for which both the rotational energy loss,  $\dot{E}_{\text{rot}}$ , and the X-ray luminosity,  $L_x$ , have been measured, there appears to be a correlation between these two quantities. This correlation appears to hold over a wide range of rotational energy losses, including different emission mechanisms of the pulsar. Since in the high  $L_x$  regime (young pulsars) of interest here the X-ray luminosity is dominated by rotational energy losses, the most appropriate energy band for our study is above  $\sim 2$  keV, where the contribution of surface emission due to the internal energy of the star is small. The correlation between  $L_x$  and  $\dot{E}_{\text{rot}}$  in the 2-10 keV band was first examined by Saito et al. (1997) for a small sample of pulsars, and a more comprehensive investigation with the largest sample up to date was later performed by P02. They found, for a sample of 39 pulsars, that the best fit is described by the relation

$$\log L_{x,[2-10]} = 1.34 \log \dot{E}_{\text{rot}} - 15.34, \quad (1)$$

with  $1\sigma$  uncertainty intervals on the parameters  $a = 1.34$  and  $b = 15.34$  given by  $\sigma_a = 0.03$  and  $\sigma_b = 1.11$ , respectively. A similar analysis on a subsample of 30 pulsars with ages  $\tau < 10^6$  yr by Guseinov et al. (2004) yielded a best fit with parameters  $a = 1.56$ ,  $b = 23.4$ , and corresponding uncertainties  $\sigma_a = 0.12$  and  $\sigma_b = 4.44$ . The slope of this latter fit is a bit steeper than that of P02; as a result, the model by Guseinov et al. predicts a larger fraction of high luminosity pulsars from the population of fast rotating young stars with respect to the best fit of P02. In order to be on the conservative side for the predicted number of high- $L_x$  pulsars, we will use as our working model the one by P02. It is interesting to note, however, that both groups find that the efficiency  $\eta_x \equiv L_x/\dot{E}_{\text{rot}}$  is an increasing function of the rotational energy loss  $\dot{E}_{\text{rot}}$  of the star. Furthermore, the analysis by Guseinov et al. shows that, for a given  $\dot{E}_{\text{rot}}$ , pulsars with larger  $B$  field have a systematically larger efficiency  $\eta_x$  of conversion of rotational energy into X-rays. An increase of  $\eta_x$  with  $\dot{E}_{\text{rot}}$  was found also in the investigation by Cheng, Taam & Wang (2004). They considered a sample of 23 pulsars and studied the trend with  $\dot{E}_{\text{rot}}$  of the pulsed and non-pulsed components separately. Their best-fit yielded  $L_x^{\text{pul}} \propto \dot{E}_{\text{rot}}^{1.2 \pm 0.08}$  for the pulsed component, and  $L_x^{\text{npul}} \propto \dot{E}_{\text{rot}}^{1.4 \pm 0.1}$  for the non-pulsed one. They noticed how the former is consistent with the theoretical X-ray magnetospheric emission model by Cheng & Zhang (1999), while the latter is consistent with a PWN model in which  $L_x^{\text{npul}} \propto \dot{E}_{\text{rot}}^{p/2}$ , where  $p \sim 2 - 3$  is the powerlaw index of the electron energy distribution. Their best fit for the total X-ray luminosity (pulsed plus unpulsed components) yielded  $L_x \propto \dot{E}_{\text{rot}}^{1.35 \pm 0.2}$ , fully consistent with the best-fit slope of P02. Along similar lines, recently Li et al. (2007) presented another statistical study in which, using *Chandra* and *XMM* data of galactic sources, they were able to resolve the component of the X-ray luminosity due to the pulsar from that due to the PWN. Their results were very similar to those of Cheng et al. (2004), with a best fit for the pulsar component  $L_x^{\text{psr}} \propto \dot{E}_{\text{rot}}^{1 \pm 0.1}$ , and a best fit for the PWN (representing the unpulsed contribution)  $L_x^{\text{PWN}} \propto \dot{E}_{\text{rot}}^{1.4 \pm 0.2}$ . They found that the main contribution to the total luminosity generally comes from the unpulsed PWN, hence yielding

the steepening of the  $L_x - \dot{E}_{\text{rot}}$  correlation with  $\dot{E}_{\text{rot}}$ , consistently with the P02 relation, where the contribution from the pulsar and the PWN are not distinguished. For our purposes, we consider the sum of both contributions, since we cannot resolve the two components in the observed sample of historical SNe.<sup>10</sup>

It should be noted that, despite the general agreement among the various studies on the trend of  $L_x$  with  $\dot{E}_{\text{rot}}$ , and the support from theory that the correlation is expected to steepen with  $\dot{E}_{\text{rot}}$ , there must be a point of saturation in order to always satisfy the condition  $L_x \leq \dot{E}_{\text{rot}}$ . While in our simulations we impose the extra condition that  $\eta_x \leq 1$ , it is clear that, until the correlation can be calibrated through direct measurements of objects with high values of  $\dot{E}_{\text{rot}}$ , there remains an uncertainty on how precisely the saturation occurs, and this uncertainty is unavoidably reflected in the precise details of our predictions. However, unless there is, for some reason, a point of turnover above the observed range where the efficiency of conversion of rotational energy into X-rays turns back into  $\eta_x \ll 1$ , then our general conclusions can be considered robust. In our analysis, in order to quantify the uncertainty associated with the above, we will also explore the consequences of a break in  $\eta_x$  just above the observed range (to be mostly conservative).

Another point to note is that one implicit assumption that we make in applying the  $L_x - \dot{E}_{\text{rot}}$  relation to very young objects is that the synchrotron cooling time  $t_{\text{synch}}$  in X-rays is much smaller than the age of the source, so that the X-ray luminosity is essentially an instantaneous tracer of  $\dot{E}_{\text{rot}}$ . In order to check the validity of this assumption, we have made some rough estimates based on measurements in known sources. For example, let's consider the case of the PWN in SN 1986J. Although the field in the PWN has not been directly measured, we can use radio equipartition and scale it from that of the Crab Nebula. The Crab's radio synchrotron emission has a minimum energy of  $\sim 6 \times 10^{48}$  ergs (see e.g. Chevalier 2005), and a volume of  $\sim 5 \times 10^{56}$  cm<sup>3</sup>. The average magnetic field is then  $\sim 550$   $\mu$ G. We can then scale to the PWN in SN 1986J, using the fact that the radio luminosity is related to that of the Crab by  $L_{r,1986J} \sim 200L_{r,\text{Crab}}$ , while its size is about 0.01 times that of the Crab. According to equipartition,  $B_{\text{min}} \sim (\text{size})^{-6/7} L_r^{2/7}$  (e.g. Willott et al. 1999), so this very crude approach suggests that the magnetic field in the PWN of SN 1986J is  $B_{\text{min}} \sim 235B_{\text{Crab}} \sim 120$  mG. This yields a very short cooling time in X-rays,  $t_{\text{synch}} \sim 5$  hr (assuming a Lorentz factor for the electrons of  $\sim 10^6$ ), so that, if we scale from the Crab nebula, the use of  $L_x - \dot{E}_{\text{rot}}$  at early times appears reasonable. If, on the other hand, initial periods are generally slower than for the Crab, then the equipartition energy could be much smaller and the corresponding lifetimes much longer. Let's then consider a  $10^{12}$  G pulsar with an initial period of 60 ms (the pulsar produced in SN 386 is such a source). We then have  $\dot{E}_{\text{rot}} \sim 3 \times 10^{36}$  erg/s, so that (ignoring expansion losses), the energy deposited in the PWN over 20 years would be  $\sim 2 \times 10^{45}$  ergs. For a volume similar to that for SN 1986J above, the equiparti-

<sup>10</sup> For typical distances  $\gtrsim$  a few Mpc, the ACIS spatial resolution is  $\gtrsim 20$  pc, while PWN sizes are on the order of a fraction of a pc to a few pc.

tion magnetic field would be  $\sim 10$  mG, corresponding to a lifetime at 2 keV of about 10 days. This is still a short enough lifetime for our purposes. Alternatively, for  $P_0 \sim 5$  ms and  $B \sim 10^{12}$  G, we have  $\dot{E}_{\text{rot}} \sim 6 \times 10^{40}$  erg/s, and over 20 years, this yields  $E_{\text{tot}} \sim 4 \times 10^{49}$  ergs. This implies  $B > 1$  G, so that  $t_{\text{synch}} \sim 15$  minutes. Therefore, we conclude that, overall, the magnetic fields in young PWNe are likely strong enough to justify the use of the  $L_x - \dot{E}_{\text{rot}}$  relation even for the youngest objects in our sample.

One further point to notice with respect to the  $L_x - \dot{E}_{\text{rot}}$  correlation is the fact that it is based on a diversity of objects. The low end range of the relation, in particular, is populated with Millisecond Pulsars (MSPs), which are spun up neutron stars. It is possible that this class of objects might bias the correlation of the youngest, isolated pulsars in the sample. Generally speaking, once they are spun up, the MSPs form PWNe again (e.g. Cheng et al. 2006), and the conversion of  $\dot{E}_{\text{rot}}$  into  $L_x$ , which is practically an instantaneous relationship (as compared to the ages under consideration), should not be dependent on the history of the system. The magnetic field of the objects (lower for the MSPs than for the young, isolated pulsars), however, might influence the conversion efficiency (Guseinov et al. 2004), hence biasing the overall slope of the correlation. Overall, in our analysis a steeper slope would lead to tighter limits on the NS spin birth distribution, and viceversa for a shallower slope. What would be affected the most by a slope change is the high  $\dot{E}_{\text{rot}}$  tail of the population. Hence, in §4, besides deriving results using the  $L_x - \dot{E}_{\text{rot}}$  for all the pulsars, we will also examine the effects of a change of slope for the fastest pulsars.

The rotational energy loss of the star, under the assumption that it is dominated by magnetic dipole losses, is given by

$$\dot{E}_{\text{rot}} = \frac{B^2 \sin^2 \theta \Omega^4 R^6}{6c^3}, \quad (2)$$

where  $R$  is the NS radius, which we take to be 10 km,  $B$  the NS magnetic field,  $\Omega = 2\pi/P$  the star angular velocity, and  $\theta$  the angle between the magnetic and spin axes. We take  $\sin \theta = 1$  for consistency with what generally assumed in pulsar radio studies. With  $\sin \theta = 1$  and a constant  $B$  field, the spin evolution of the pulsars is simply given by

$$P(t) = \left[ P_0^2 + \left( \frac{16\pi^2 R^6 B^2}{3Ic^3} \right) t \right]^{1/2}, \quad (3)$$

where  $I \approx 10^{45} \text{ g cm}^2$  is the moment of inertia of the star, and  $P_0$  is its initial spin period. The X-ray luminosity of the pulsar at time  $t$  (which traces  $\dot{E}_{\text{rot}}$ ) correspondingly declines as  $L_x = L_{x,0}(1 + t/t_0)^{-2}$ , where  $t_0 \equiv 3Ic^3 P_0^2 / B^2 R^6 (2\pi)^2 \sim 6500 \text{ yr } I_{45} B_{12}^{-2} R_{10}^{-6} P_{0,10}^2$ , having defined  $I_{45} \equiv I / (10^{45} \text{ g cm}^2)$ ,  $R_{10} \equiv R / (10 \text{ km})$ ,  $P_{0,10} \equiv P_0 / (10 \text{ ms})$ . For  $t \lesssim t_0$  the flux does not vary significantly. Since the ages  $t_{\text{SN}}$  of the SNe in our sample are all  $\lesssim 77$  yr, we deduce that, for typical pulsar fields,  $t_{\text{SN}} \ll t_0$ . The luminosities of the pulsars associated with the SNe in our sample are therefore expected to be still in the plateau region, and thus they directly probe the initial birth parameters, before evolution affects the periods appreciably.

In order to compute the X-ray luminosity distribution of a population of young pulsars, the magnetic fields and the initial periods of the pulsars need to be known. As dis-

cussed in §1, a number of investigations have been made over the last few decades in order to infer the birth parameters of NSs, and in particular the distribution of initial periods and magnetic fields. Here, we begin our study by comparing the SN data with the results of a pulsar population calculation that assumes one of such distributions, and specifically one that makes predictions for birth periods in the millisecond range. After establishing that the SN data are highly inconsistent with such short initial spins, we then generalize our analysis by inverting the problem, and performing a parametric study aimed at finding the minimum values of the birth periods that result in predicted X-ray luminosities consistent with the SN X-ray data.

#### 4 OBSERVATIONAL CONSTRAINTS ON THE PULSAR X-RAY LUMINOSITIES FROM COMPARISON WITH HISTORICAL SNE

As a starting point to constrain pulsar birth parameters, we consider the results of one of the most recent and comprehensive radio studies, based on large-scale radio pulsar surveys, that is the one carried out by Arzoumanian et al. (2002; ACC in the following). They find that, if spin down is dominated by dipole radiation losses (i.e. braking index equal to 3), and the magnetic field does not appreciably decay, the magnetic field strength (taken as Gaussian in log) has a mean  $\langle \log B_0 [G] \rangle = 12.35$  and a standard deviation of 0.4, while the initial birth period distribution (also taken as a log-Gaussian), is found to have a mean  $\langle \log P_0 (s) \rangle = -2.3$  with a standard deviation  $\sigma_{P_0} > 0.2$  (within the searched range of 0.1 – 0.7). In the first part of our paper, as a specific example of a distribution that predicts a large fraction of pulsars to be born with millisecond periods, we use their inferred parameters described above. Since in their model the standard deviation for the initial period distribution is constrained only by the lower limit  $\sigma_{P_0} > 0.2$ , here we adopt  $\sigma_{P_0} = 0.3$ . As the width of the velocity dispersion increases, the predicted X-ray luminosity distribution becomes more and more heavily weighed towards higher luminosities (see Figure 1 in Perna & Stella 2004). Therefore, the limits that we derive in this section would be even stronger if  $\sigma_{P_0}$  were larger than what we assume. We then assume that the  $L_x - \dot{E}_{\text{rot}}$  correlation is described by the P02 best fit with the corresponding scatter.

In order to test the resulting theoretical predictions for the pulsar distribution of X-ray luminosities against the limits of the SNe, we perform  $10^6$  Monte Carlo realizations of the compact object remnant population. Each realization is made up of  $N_{\text{obj}} = N_{\text{SN}} = 100$ , with ages equal to the ages of the SNe in our sample. The fraction of massive stars that leave behind a black hole (BH) has been theoretically estimated in the simulations by Heger et al. (2003). For a solar metallicity and a Salpeter IMF, they find that this fraction is about 13% of the total. However we need to remark that while, following their predictions, in our Monte Carlo simulations we assign a 0.13 probability for a remnant to contain a BH, the precise BH fraction is, in reality, subject to a certain degree of uncertainty. Even taking rigorously the results of Heger et al. (2003), one needs to note that their NS vs BH fraction (cfr. their fig.5) was computed assuming a fraction of about 17% of Type Ib/c SNe, and 87% of Type II. Our

sample, on the other hand, contains about 40% of Type Ib/c and 60% of Type II SNe. How the remnant fraction would change in this case is difficult to predict. Heger et al. point out how normal Type Ib/c SNe are not produced by single stars until the metallicity is well above solar. In this case, the remnants would be all NSs. At lower metallicities, on the other hand, most Type Ib/c SNe are produced in binary systems where the binary companion helps in removing the hydrogen envelope of the collapsing star. Given these uncertainties, while adopting for our simulations the BH/NS fraction estimated by Heger et al. for solar metallicity, we also discuss how results would vary for different values of the BH and NS components.

If an object is a BH, a low level of X-ray luminosity ( $< 10^{35}$  erg/s, i.e. smaller than the lowest measurement/limit in our SN data set) is assigned to it. This is the most conservative assumption that we can make in order to derive constraints on the luminosity distribution of the NS component. If an object is a NS, then its birth period and magnetic field is drawn from the ACC distribution as described above, and it is evolved to its current age (equal to the age of the corresponding SN at the time of the observation) with Eq.(3). The corresponding X-ray luminosity is then drawn from a log-Gaussian distribution with mean given by the P02 relation, and dispersion  $\sigma_{L_x} = \sqrt{\sigma_a^2 [\log \dot{E}_{\text{rot}}]^2 + \sigma_b^2}$ .

Figure 1 (top panel) shows the predicted distribution of the most frequent value<sup>11</sup> of the pulsar luminosity over all the Monte Carlo realizations of the entire sample of Table 1. The shaded region indicates the  $1\sigma$  dispersion in the model. This has been determined by computing the most compact region containing 68% of the random realizations of the sample. Also shown is the distribution of the X-ray luminosity (both detections and upper limits) of the SNe (cfr. Table 1). Since the measured X-ray luminosity of each object is the sum of that of the SN itself and that of the putative pulsar embedded in it, for the purpose of this work X-ray detections are also treated as upper limits on the pulsar luminosities. This is indicated by the arrows in Figure 1.

Our X-ray analysis, in all those cases where a measurement was possible, never revealed column densities high enough to affect the observed 2-10 keV flux significantly. However, if a large fraction of the X-ray luminosity (when not due to the pulsar) does not come from the innermost region of the remnant, then the inferred  $N_{\text{H}}$  would be underestimated with respect to the total column density to the pulsar. The total optical depth to the center of the SN as a function of the SN age depends on a number of parameters, the most important of which are the ejected mass and its radial distribution. The density profile of the gas in the newly born SN is determined by the initial stellar structure, as modified by the explosion. Numerical simulations of supernova explosions produce density distributions that, during the free expansion phase, can be approximated by the functional form  $\rho_{\text{SN}} = f(v)t^{-3}$  (see e.g. Chevalier & Fransson 1994 and references therein). The function  $f(v)$  can in turn

<sup>11</sup> For each (binned) value of the pulsar luminosity, we determined the corresponding probability distribution resulting from the Monte Carlo simulations. The maximum of that distribution is what we indicated as the “most frequent” value for each bin.

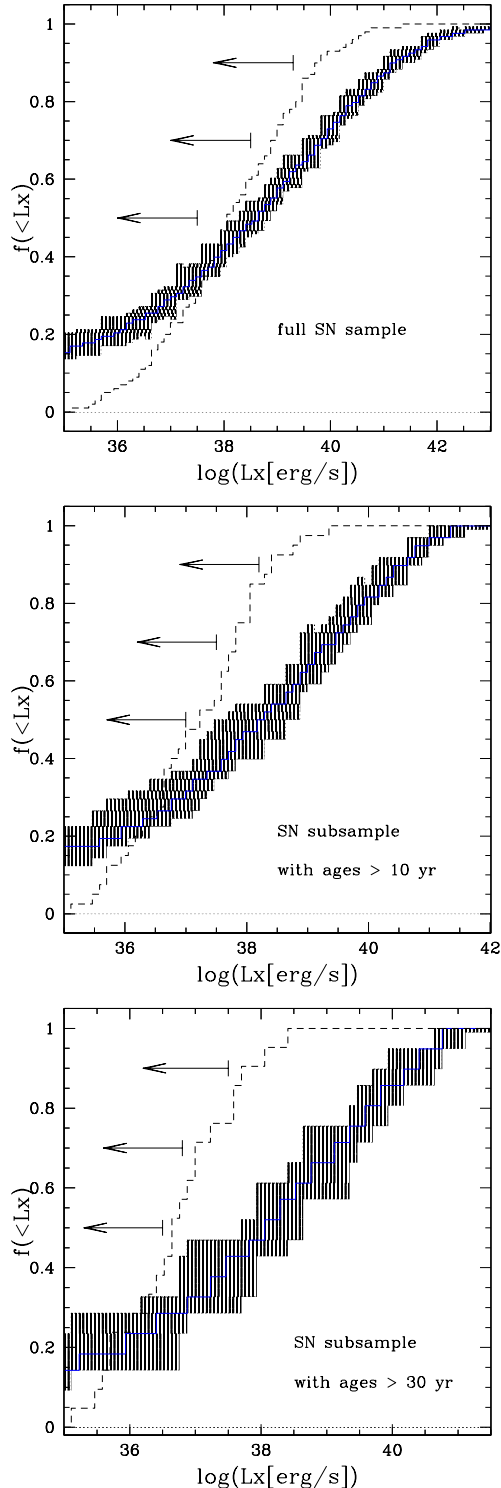


**Figure 1.** The dashed line shows the distribution of 2-10 keV luminosities (either measurements or upper limits) for the entire sample of 100 SNe analyzed (*upper panel*), for the subsample of SNe with ages  $> 10$  yr (*middle panel*), and with ages  $> 30$  yr (*lower panel*). The measured SN luminosities are also treated as upper limits on the luminosities of the embedded pulsars. The solid line shows the prediction for the X-ray luminosity distribution of pulsars born inside those SNe, according to the ACC birth parameters and the  $L_X - \dot{E}_{\text{rot}}$  P02 relation. The shaded regions indicate the  $1-\sigma$  confidence level of the model, derived from  $10^6$  random realizations of the sample. Independently of the SN sample considered, the pulsar luminosity distribution is highly inconsistent with the corresponding SN X-ray limits.

be represented by a power-law in velocity,  $f(v) \propto v^{-n}$ . To date, the best studied case is that of SN 1987A. Modeling by Arnett (1988) and Shigeyama & Nomoto (1990) yield an almost flat inner powerlaw region, surrounded by a very steep outer powerlaw profile,  $n \sim 9 - 10$ . For normal abundances and at energies below<sup>12</sup> 10 keV, Chevalier & Fransson (1994) estimate the optical depth at energy  $E_{10} \equiv E/(10 \text{ keV})$  to the center of a supernova with a flat inner density profile to be  $\tau = \tau_s E_{10}^{-8/3} E_{\text{SN},51}^{-3/2} M_{\text{ej},10}^{5/2} t_{\text{yr}}^{-2}$ , where  $E_{\text{SN},51}$  is the supernova energy in units of  $10^{51}$  erg, and  $M_{\text{ej},10}$  is the mass of the ejecta in units of  $10 M_{\odot}$ . The constant  $\tau_s$  is found to be 5.2 for a density profile with  $n = 7$  in the outer parts, and 4.7 for  $n = 12$ . From these simple estimates, it can be seen that the SN would have to wait a decade or so before starting to become optically thin at the energies of interest. These estimates however do not account for the fact that, if the SN harbors an energetic pulsar in its center, the pulsar itself will ionize a substantial fraction of the surrounding neutral material. Calculations of the ionization front of a pulsar in the interior of a young SN were performed by Chevalier & Fransson (1992). In the case of a flat density profile in the inner region, and an outer density profile with powerlaw  $n = 9$ , they estimate that the ionization front reaches the edge of the constant density region after a time  $t_{\text{yr}} = 10 t_0 f_i^{-1/3} \dot{E}_{\text{rot},41}^{-1/3} M_{\text{ej},10}^{7/6} E_{\text{SN},51}^{-1/2}$ , where  $\dot{E}_{\text{rot},41} \equiv \dot{E}_{\text{rot}}/10^{41} \text{ erg s}^{-1}$ , and  $f_i$  is the fraction of the total rotational power that is converted in the form of ionizing radiation with a mean free path that is small compared to the supernova size. The constant  $t_0$  depends of the composition of the core. For a hydrogen-dominated core,  $t_0 = 1.64$ , for a helium-dominated core,  $t_0 = 0.69$ , and for an oxygen-dominated core  $t_0 = 0.28$ . Once the ionization front has reached the edge of the constant density region, the steep outer power-law part of the density profile is rapidly ionized. Therefore, depending on the composition and total mass of the ejecta, an energetic pulsar can ionize the entire mass of the ejecta on a timescale between a few years and a few tens of years. This would clearly reduce the optical depth to the center of the remnant estimated above.

Given these considerations, in order to make predictions that are not as likely to be affected by opacity effects, we also performed a Monte Carlo simulation of the compact remnant population for all the SNe with ages  $t > 10$  yr, and another for all the SNe with ages  $t > 30$  yr. Since the opacity scales as  $t^{-2}$ , these subsets of objects are expected to be substantially less affected by high optical depths to their inner regions. The subsample of SNe with ages  $t > 10$  yr contains 40 objects, while the subsample with ages  $t > 30$  yr contains 21 SNe. The corresponding luminosity distributions (both measurements and limits) are shown in Figure 1 (middle and bottom panel respectively), together with the predictions of the adopted model (ACC initial period distribution and P02  $L_x - \dot{E}_{\text{rot}}$  correlation) for the luminosities of the pulsars associated with those SN samples. Given the uncertainties in the early-time optical depth, we consider the constraints derived from these subsamples (and especially the one with  $t > 30$  yr) more reliable. Furthermore, even independently of optical depth effects that can bias the youngest mem-

bers of the total sample, the subsamples of older SNe have on average lower luminosities, hence making the constraints on the model predictions more stringent. In the following, when generalizing our study to derive limits on the allowed initial period distribution, we will use for our analysis only the subsets of older SNe.

In all three panels of Figure 1, the low luminosity tail of the simulation, accounting for  $\sim 15\%$  of the population, is dominated by the fraction of SNe whose compact remnants are black holes, and for which we have assumed a luminosity lower than the lowest SN measurement/limit ( $\sim 10^{35}$  erg/s). While it is possible that newly born BHs could be accreting from a fallback disk and hence have luminosities as high as a few  $\times 10^{38}$  erg/s, our assumption of low luminosity for them is the most conservative one for the analysis that we are performing, in that it allows us to derive the most stringent limits on the luminosity of the remaining remnant population of neutron stars. For these, the high-luminosity tail is dominated by the fastest pulsars, those born with periods of a few ms. The magnetic fields, on the other hand, are in the bulk range of  $10^{12} - 10^{13}$  G. The low- $B$  field tail produces lower luminosities at birth, while the high- $B$  field tail will cause the pulsars to slow down on a timescale smaller than the typical ages of the SNe in the sample. Therefore, it is essentially the initial periods which play a crucial role in determining the extent of the high-luminosity tail of the distribution. With the birth parameter distribution used here, we find that, out of the  $10^6$  Monte Carlo realizations of the sample (for each of the three cases of Fig.1), none of them predicts pulsar luminosities compatible with the SN X-ray limits.<sup>13</sup>

These results point in the direction of initial periods of the pulsar population to be slower than the ms periods derived from some population synthesis studies in the radio. A number of other investigations in the last few years, based on different methods of analysis of the radio sample with respect to ACC, have indeed come up to conclusions similar to ours. The population synthesis studies of Faucher-Giguere & Kaspi (2005) yielded a good fit to the data with the birth period described by a Gaussian with a mean period of 0.3 s and a spread of 0.15 sec. Similarly, the analysis by Ferrario & Wickramasinghe (2006) yielded a mean period of 0.23 sec for a magnetic field of  $10^{12}$  G. We performed Monte Carlo simulations of the X-ray pulsar population using the birth parameters derived in those studies above, and found them to be consistent with the SNe X-ray limits shown in Figure 1.

In order to generalize our analysis beyond the testing of known distributions, we performed a number of Monte Carlo simulations with different initial spin period distributions and a mean magnetic field given by the optimal model of Faucher-Giguere & Kaspi (2006). This is a log-Gaussian with mean  $\langle \log(B/\text{G}) \rangle = 12.65$  and dispersion  $\sigma_{\log B} = 0.55$ .<sup>14</sup>

<sup>13</sup> We need to point out that, in the study presented here, we refrain from performing detailed probability analysis. This is because, given the observational uncertainties of some of the input elements needed for our study (as discussed both above and in the following), precise probability numbers would not be especially meaningful at this stage.

<sup>14</sup> The inferred values of the magnetic field in different studies are all generally in this range, even for very different inferred spin birth parameters. Furthermore, Ferrario & Wickramasinghe

<sup>12</sup> Above 10 keV, the opacity is dominated by electron scattering, which is energy independent.

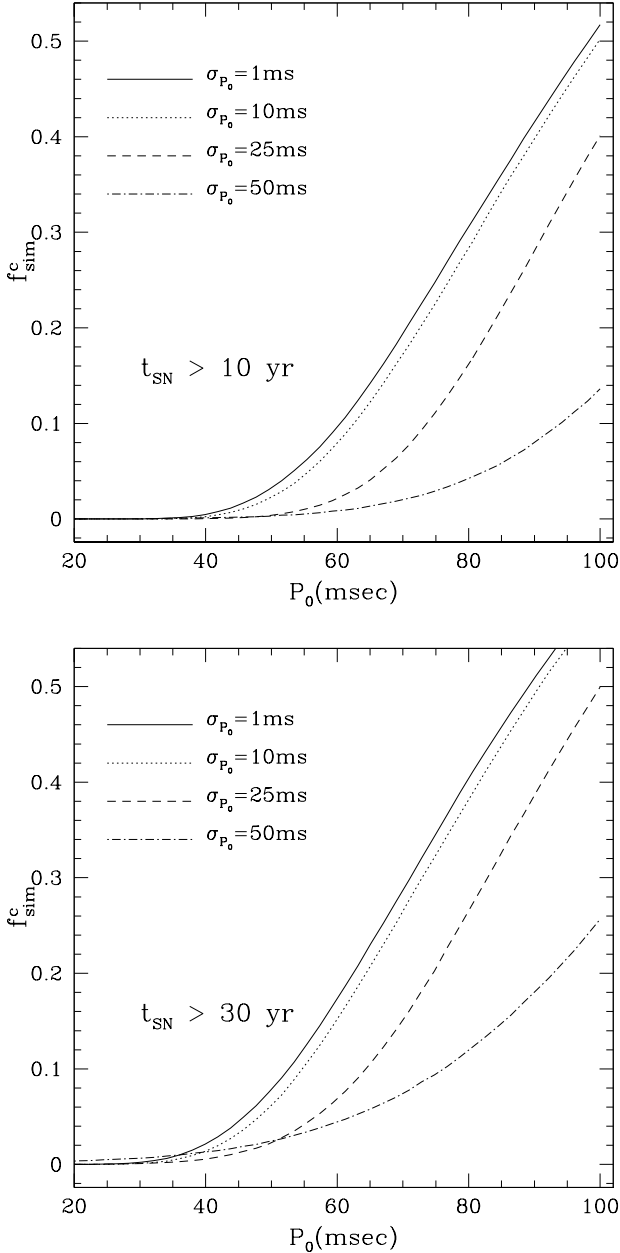


**Figure 2.** Fraction  $f_{sim}^c$  of Monte Carlo realizations of the SN sample for which the 2-10 keV luminosities of the pulsars are below the limits of the corresponding SNe. This is shown for different distributions of the initial spin periods, described by Gaussians of mean  $P_0$  and dispersion  $\sigma_{P_0}$ . In the upper panel, the sample includes only the SNe of ages  $> 10$  yr (cfr. Fig.1, middle panel), while in the lower panel only the SNe with ages  $> 30$  yr (cfr. Fig.1, lower panel) are included for the montecarlo simulations. Independently of the sample considered, initial periods  $P_0 \lesssim 40$  ms are inconsistent with the SN data.

Figure 2 shows the fraction  $f_{sim}^c$  of the montecarlo simulations of the SN sample for which the luminosity of each

(2006) note that the pulsar birth period that they infer is almost independent of the field value in the range  $\log B(\text{G}) = 10 - 13$ , where the vast majority of isolated radio pulsars lie.

pulsar is found below that of the corresponding SN. The sample of SNe selected is either the one with ages  $> 10$  yr (top panel), or the one with ages  $> 30$  yr (bottom panel), which allow tighter constraints while minimizing optical depth effects. Monte Carlo realizations of the samples have been run for 50 Gaussian distributions of the period with mean in the range  $20 - 100$  ms, and, for each of them, 4 values of the dispersion<sup>15</sup>  $\sigma_{P_0}$  between 1 and 50 ms. For each value of the period, we performed 100,000 random realizations<sup>16</sup>. Details of the results vary a bit between the two age-limited subsamples. This is not surprising since the extent to which we can draw limits on the pulsar periods depends on the measurements/limits of the X-ray luminosities of the SNe in the sample. In a large fraction of the cases, we have only upper limits, and therefore our analysis is dependent on the sensitivity at which each object has been observed. Independently of the sample, however, we find that, for initial periods  $P_0 \lesssim 35 - 40$  ms, the distribution of pulsar luminosities is highly inconsistent with the SN data for any value of the assumed width of the period distribution.

We need to emphasize that the specific value of  $f_{sim}^c$  as a function of  $P_0$  should be taken as representative. Various authors have come up with slightly different fits for the  $L_x - \dot{E}_{rot}$  correlation. If, for example, instead of the fit by Possenti et al. (2002) we had used the fit derived by Gusseinov et al. (2004), then the limits on the period would have been more stringent. On the other hand, if, for some reason, the efficiency  $\eta_x$  of conversion of  $\dot{E}_{rot}$  into  $L_x$  becomes low at high  $\dot{E}_{rot}$ , then our results would be less constraining. In order to assess the robustness of our results with respect to changes in  $\eta_x$ , we ran simulations of the pulsar population assuming that, for  $\dot{E}_{rot} > \dot{E}_{rot}^{\text{max,obs}} \sim 10^{39}$  erg s<sup>-1</sup> (where  $\dot{E}_{rot}^{\text{max,obs}}$  is the maximum observed  $\dot{E}_{rot}$ ), the efficiency becomes  $\eta'_x = \epsilon \eta_x$ , and we tried with a range of values of  $\epsilon < 1$ . This test also addresses the issue of a bias in our results deriving from a possible shallower slope for the youngest pulsars of the population, as discussed in §3. We ran Monte Carlo simulations for the ACC birth parameters, and decreased  $\epsilon$  by increments of 0.02. We found that, only for the very low value  $\epsilon \sim 10^{-4}$ , a sizable fraction of  $\sim 5\%$  of the simulations predicts pulsar X-ray luminosities that are fully consistent with the SN data. Therefore, we conclude that our results on the millisecond birth periods of pulsars are reasonably robust with respect to uncertainty in the  $L_x - \dot{E}_{rot}$  for the youngest members of the population.

Another systematic that might in principle affect our results would arise if a fraction of neutron stars is born with a non-active magnetosphere so that their X-ray luminosity at high  $\dot{E}_{rot}$  is much smaller than for the active pulsars,

<sup>15</sup> The dependences with  $\sigma_{P_0}$  should be taken as representative of the general trend, since it is likely that  $\sigma_{P_0}$  and  $P_0$  might be correlated. But since no such correlations have been studied and reported, we took as illustrative example the simplest case of a constant  $\sigma_{P_0}$  for a range of  $P_0$ .

<sup>16</sup> The number of random realizations is smaller here with respect to Fig.1 for computational reasons since, while each panel of Fig.1 displays a Monte Carlo simulation for one set of parameters only, each panel of Fig. 2 is the results of 200 different Monte Carlo realizations. For a few cases, however, we verified that the results were statistically consistent with those obtained with a larger number of random realizations.

then the limits on the initial periods of the “active” pulsars would be less stringent. An example of non-active neutron stars could be that of the CCOs discussed in §3. However, until the fraction of these stars becomes well constrained by the observations and an independent  $L_x - \dot{E}_{\text{rot}}$  is established for them, it is not possible to include them quantitatively in our population studies. Similarly, the precise fraction of BHs versus NSs in the remnant population plays a role in our results. A larger fraction of BHs would alleviate our constraints on the initial spin periods, while a smaller fraction would, obviously, make them tighter. If a fraction of those BHs had a luminosity larger than the maximum assumed upper limit in our simulations (due to e.g. accretion from a fall-back disk as discussed above), then our results would again be more constraining. While our work is the first of its kind in performing the type of analysis that we present, future studies will be able to improve upon our results, once the possible systematics discussed above are better constrained, and deeper limits are available for the full SN sample.

## 5 SUMMARY

In this paper we have proposed a new method for probing the birth parameters and energetics of young neutron stars. The idea is simply based on the fact that the X-ray measurements of young supernovae provide upper limits to the luminosity of the young pulsars embedded in them. The pulsar X-ray luminosity on the other hand, being directly related to its energy loss, provides a direct probe of the pulsar spin and magnetic field. Whereas pulsar birth parameters are generally inferred through the properties of the radio population, the X-ray properties of the youngest members of the population provide tight and independent constraints on those birth parameters, and, as we discussed, especially on the spins.

The statistical comparison between theoretical predictions and the distribution of X-ray luminosity limits that we have performed in this work has demonstrated that the two are highly inconsistent if the bulk of pulsars is born with periods in the millisecond range. Whereas we cannot exclude that the efficiency  $\eta_x$  of conversion of rotational energy into X-ray luminosity could have a turnover and drop at high values of  $\dot{E}_{\text{rot}}$  to become  $\eta_x \ll 1$ , the 2-10 keV pulsar data in the currently observed range of  $\dot{E}_{\text{rot}}$  do not point in this direction (but rather point to an increase of  $\eta_x$  with  $\dot{E}_{\text{rot}}$ ), and there is no theoretical reason for hypothesizing such a turn over. However, even if such a turnover were to exist just above the observed range of  $\dot{E}_{\text{rot}}$ , we found that only by taking an efficiency  $\eta'_x \sim 10^{-4} \eta_x$  above  $\dot{E}_{\text{rot}}^{\text{max,obs}}$ , our results would lose their constraining value for the ms spin birth distributions. Therefore, we can robustly interpret our results as an indication that there must be a sizable fraction of pulsars born with spin periods slower than what has been derived by a number of radio population studies as well as by hydrodynamic simulations of SN core-collapse (e.g. Ott et al 2006). Our findings go along the lines of a few direct measurements of initial periods of pulsars in SNRs (see e.g. Table 2 in Migliazzo et al. 2002), as well as some other population synthesis studies (Faucher-Giguère & Kaspi 2006; Ferrario & Wickramasinghe 2006; Lorimer et al. 2006). Our results for the bulk of the pulsar population, however, do not

exclude that the subpopulation of magnetars could be born with very fast spins, as needed in order to create the dynamo action responsible for the  $B$ -field amplification required in these objects (Thompson & Duncan 1993). Because of their very short spin-down times, the energy output of magnetars can be dominated by the spin down luminosity only up to timescales of a fraction of year, during which the SN is still too optically thick to let the pulsar luminosity go through. Therefore, our analysis cannot place meaningful constraints on this class of objects.

Finally, our results also bear implications on the contribution of young pulsars to the population of the Ultra Luminous X-ray sources (ULXs) observed in nearby galaxies. The model in §3 predicts that a sizable fraction of that population could indeed be made up of young, fast rotating pulsars (Perna & Stella 2004). However, the analysis performed here shows that the contribution from this component, although expected from the tail of the population, cannot be as large as current models predict.

The extent to which we could perform our current analysis has been limited by the size of the SNe sample, and, especially, by the available X-ray measurements. The fact that, in a large fraction of the sample, we have limits rather than detections, means that a large improvement can be made with deeper limits from longer observations. The deeper the limits, the tighter the constraints that can be derived on the spin period distribution of the pulsars. The analysis proposed and performed here is completely uncorrelated from what done in radio studies, and therefore it provides an independent and complementary probe of the pulsar spin distribution at birth (or shortly thereafter); our results provide stronger constraints on theoretical models of stellar core collapse and early neutron star evolution, making it even more necessary to explain why neutron stars spin down so rapidly immediately after birth (see also Thompson, Chang & Quataert 2004; Metzger, Thompson & Quataert 2007).

## ACKNOWLEDGEMENTS

We thank Roger Chevalier, John Raymond and Stefan Immler for very useful discussions on several aspects of this project. We are especially grateful to Bryan Gaensler and Shami Chatterjee for their careful reading of our manuscript and detailed comments. We also thank the referee for his/her insightful suggestions. RP and RS thank the University of Sydney for the partial support and the kind hospitality during the initial phase of this project.

## REFERENCES

- Arnaud, K. A. 1996, in “Astronomical Data Analysis Software and Systems V”, A.S.P. Conference Series, Vol. 101, 1996, George H. Jacoby and Jeannette Barnes, eds., p. 17
- Arnett, W. D. 1988, *ApJ*, 331, 377
- Arzoumanian, Z., Cordes, J. M., & Chernoff, D. F. 2002, *ApJ*, 568, 289 (ACC)
- Bandiera, R., Pacini, F. & Salvati, M. 1984, *ApJ*, 285, 134
- Bartel, N. & Bietenholz, M. 2005, *Adv. Space Res.*, 35, 1057
- Becker, W. & Trumper, J. 1997, *A&A*, 326, 682
- Blaes, O. & Madau, P. 1993, *ApJ*, 403, 690
- Chatterjee, P., Hernquist, L., & Narayan, R. 2000, *ApJ*, 534, 373

- Chevalier, R. 1987, *Nature*, 329, 611
- Chevalier, R. A. 1989, *ApJ*, 346, 847
- Chevalier, R. A. 1995, *ApJ*, 619, 839
- Chevalier, R. & Fransson, C. 1992, *ApJ*, 395, 540
- Chevalier, R. & Fransson, C. 1994, *ApJ*, 420, 268
- Cheng, K. S. & Zhang, L. 1999, *ApJ*, 515, 337
- Cheng, K. S., Taam, R. E. & Wang, W. 2004, *ApJ*, 617, 480
- Cheng, K. S., Taam, R. E. & Wang, W. 2006, *ApJ*, 641, 427
- Colgate, S. A. 1971, *ApJ*, 163, 221
- Cordes, J. M. & Chernoff, D. F. 1998, *ApJ*, 505, 315
- Dall’Osso, S. & Stella, L. 2007, *Astrophysics and Space Science*, 308, 119
- Emmering, R. T. & Chevalier, R. A. 1989, *ApJ*, 345, 931
- Fabbiano, G. & White, N. 2003, in “Compact Stellar X-ray Sources”, Cambridge University Press (eds. W. Lewin & M. van der Klis)
- Faucher-Giguere, C.-A., & Kaspi, V. 2006, *ApJ*, 643, 355
- Ferrario, L. & Wickramasinghe, D. 2006, *MNRAS*, 367, 1323
- Gunn, J. E. & Ostriker, J. P. 1970, *ApJ*, 160, 979
- Guseinov, O. H., Ankay, A., Tagieva, S. O., Taskin, M. O. 2004, *IJMPD*, 13, 197
- Hartman, J. W., Bhattacharya, D., Wijers, R., & Verbunt, F. 1997, *A&A*, 322, 477
- Heger, A., Fryer, C. L., Woosely, S. E., Langer, N., Hartmann, D. H. 2003, *ApJ*, 591, 288
- Illarionov, A. F. & Sunyaev, R. A. 1975, *A&A*, 39, 185
- Kraft, R. P., Burrows, D. N. & Nousek, J. A. 1991, *ApJ*, 374, 344
- Li, X.-H., Lu, F.-J. & Li, Z. 2007, *ApJ* submitted, preprint astro-ph/0707.4279
- Lorimer, D. R., Bailes, M., Dewey, R. J., Harrison, P. A. 1993, *MNRAS*, 263, 403
- Lorimer, D. R. et al. 2006, *MNRAS*, 372, 77
- Lyne, A. G., Manchester, R. N. & Taylor, J. H. 1985, *MNRAS*, 213, 613
- Lundqvist, P. & Fransson, C. 1988, *A&A*, 192, 221
- Metzger, B. D., Thompson, T. A. & Quataert, E. 2007, *ApJ*, 659, 561
- Michel, F. C. 1991, in “Theory of Neutron Star Magnetosphere”, University of Chicago Press, Chicago, IL
- Michel, F. C., & Dessler, A. J. 1981, *ApJ*, 251, 654
- Migliazzo, J. M., Gaensler, B. M., Backer, D. C., Stappers, B. W., van der Swaluw, E., Strom, R. G. 2002, *ApJ*, 657L, 41
- Narayan, R. & Ostriker, J. P. 1990, *ApJ*, 352, 222
- Ott C. D., Burrows, A., Thompson, T. A., Livne, E., Walder, R. 2006, *ApJS*, 164, 130
- Pavlov, G. G., Zavlin, V. E., Aschenbach, B., Trmper, J. & D. Sanwal, D. 2000, *ApJ*, 531L, 53
- Perna, R. & Stella, L. 2004, *ApJ*, 615, 222
- Perna, R., Hernquist, L., & Narayan, R. 2000, *ApJ*, 541, 344
- Perna, R., Narayan, R., Rybicki, G., Stella, L. & Treves, A. 2003, *ApJ*, 594, 936
- Petre, R., Becker, M., Winkler, P. F. 1996, *ApJ*, 465L, 43
- Phinney, E. S. & Blandford, R. D. 1981, *MNRAS*, 194, 137
- Popov, S.B., Colpi, M., Treves, A., Lipunov, V. M., Prokhrov, M. E. 2000, *ApJ*, 530, 896
- Possenti, A., Cerutti, R., Colpi, M. & Mereghetti, S. 2002, *A&A*, 387, 993
- Ptak, A. & Colbert, E. 2004, *ApJ* in press, astro-ph/0401525
- Reynolds, S. P. & Fix, J. D. 1987, *ApJ*, 322, 673
- Rupen, M. P., van Gorkom, J. H., Knapp, G. R., Gunn, J. E., Schneider, D. P. 1987, *AJ*, 94, 61
- Saito, Y., Kawai, N., Kamae, T., Shibata, S. 1997, in “Proceedings of the Fourth Compton Symposium, Editors Charles D. Dermer, Mark S. Strickman, and James D. Kurfess, Williamsburg, VA April 1997: AIP Conference Proceedings 410, p. 628”
- Seward, F. D. & Wang, Z. 1988, *ApJ*, 332, 1999
- Shigeyama, T. & Nomoto, K. 1990, *ApJ*, 360, 242
- Stollman, G.M. 1987, *A&A*, 171, 152
- Thompson, T. A., Chang, P. & Quataert, E. 2004, *ApJ*, 611, 380
- Thompson, C. & Duncan, R. C. 1993, *ApJ*, 408, 194
- Tsvetkov, D. Yu., Pavlyuk, N. N., Bartunov, O. S. 2004, *AstL*, 30, 729
- Verbunt, F., Kuiper, L., Belloni, T., Johnston, H. M., de Bruyn, A. G., Hermsen, W., van der Klis, M. 1996, *A&A*, 311, L9
- Vranesevic, N. et al. 2004, *ApJ*, 617, L139
- Willott, C. J., Rawlings, S., Blundell, K. M., Lacy, M. 1999, *MNRAS*, 309, 1017
- Yusifov, I. M., Alpar, M. A., Gok, F., & Huseynov, O. H. 1995, in *The Lives of the Neutron Stars*, ed. M. A. Alpar, U. Kiziloglu, & J. van Paradijs (NATO ASI Ser. C, 450; Dordrecht: Kluwer), 201